Permeation of Hydrogen and Deuterium Through Palladium-Silver Alloys

FRANK J. ACKERMAN[1] and GEORGE J. KOSKINAS
Lawrence Radiation Laboratory, University of California, Livermore, Calif. 94550

Permeation of hydrogen and deuterium through palladium–25 wt % silver alloy tubes has been studied at driving pressures to 1000 psia with back pressures to 100 psia, and at temperatures of 300°, 400°, and 500°C. The data are represented by the following equations:

$$R_{H_2} = 3.85 \times 10^{-6} A \exp(-794/T)(P_H^{1/2} - P_L^{1/2})/h$$

and

$$R_{D_2} = 1.68 \times 10^{-6} A \exp(-479/T)(P_H^{1/2} - P_L^{1/2})/h$$

where R is g mol/min of H_2 or D_2; A is the effective area of membrane, cm^2; T is the temperature, °K; h is the thickness of membrane, cm; P_H is the driving pressure, psia; and P_L is the back pressure, psia.

In spite of the large amount of work done on the hydrogen–palladium system (*13*), application has been hindered both by disagreement in the results and a lack of data at driving pressures and back pressures on alloys of commercial interest. Some of the disagreement is clearly due to poisoning (*5*). The reasons for disagreement in other cases are not so clear.

Most of the existing data are for pressures below 100 psia, and little work has been published for driving pressures above 200 psia or back pressures above 1 atm. Hunter has measured the permeation of hydrogen through palladium and palladium-silver alloys at driving pressures to 800 psia and back pressures to 600 psia (*9*, *10*). For deuterium, no work above 200 psia has been found.

This paper presents permeation measurements for hydrogen and deuterium through palladium–silver membranes at the following conditions: temperature, 300–500°C, driving pressure, 100–1000 psia, and back pressure, 16–100 psia.

THEORY

The permeation of hydrogen isotopes through palladium and its alloys is believed to proceed by several steps (*13*): gas-phase diffusion of hydrogen molecules to the palladium–silver surface, adsorption of the hydrogen on the surface and dissociation into ions, solution of the hydrogen ions into the palladium–silver surface, diffusion through bulk metal, reemergence of hydrogen from solution, recombination and desorption of molecules from palladium–silver surface, and gas-phase diffusion from surface.

Several investigators have shown that the diffusion through the bulk metal is the rate-controlling step for nonpoisoned membranes 0.001 in. thick or greater (*4*, *11*). Diffusion through a solid is governed by Fick's law (*12*). For steady-state diffusion, this is expressed by:

$$R = \text{Const.} = -AD\,\frac{dc}{dx} \tag{1}$$

where R is the permeation rate, A is the effective area, D is the diffusivity, x is the diffusion path length, and c is the concentration of hydrogen in solution. Integration of Equation 1 for a cylindrical geometry with the concentration independent diffusion coefficient D gives:

$$R = AD(C_1 - C_2)/(r_1 - r_2) \tag{2}$$

where C_1 and C_2 are the concentrations at the inner radius r_1, and outer radius r_2, respectively. The effective area, A, is defined as the log mean area:

$$A = \frac{2\,\pi l(r_2 - r_1)}{\ln\,(r_2/r_1)} \tag{3}$$

where l is the length of the cylinder. Since diffusivity and solubility are complicated functions of temperature and hydrogen pressure, an empirical rate expression is often used. An empirical equation derived from Equation 2 is:

$$R = aA\exp\,(b/T)(P_H^{1/2} - P_L^{1/2})/h \tag{4}$$

where a and b are empirical constants, P_H is the driving pressure, P_L is the back pressure, and h is the wall thickness. The exponential term combines temperature dependence of both the diffusion coefficient and the solubility; therefore, b is not strictly an activation energy. The square-root relationship between solubility and pressure is Sievert's law (*17*). This equation should hold where hydrogen-isotope solubility is low; however, as noted by Hickman (*7*), at high pressures and low temperatures where the hydrogen/palladium ratio approaches 0.3, there is marked deviation of solubility from $p^{1/2}$ behavior. To represent this region, a more complicated expression is needed which reflects the saturation effects of the solubility vs. relationship, as well as the solubility dependence of the diffusion coefficient reported by Hickman (*6*). Since equation 4 adequately represents the permeation data in the range of this study, a more complicated equation was unnecessary.

EXPERIMENTAL

Equipment. A diagram of the experimental equipment is shown in Figure 1. The quantity of gas flowing into the permeation cell is calculated from the pressure P_1, and temperature, T_1, readings on the supply volume V. The pressure of the gas flowing into the cell is set by control valve C_1 and measured by P_2. The preheat coil brings the incoming gas up to temperature before it enters the palladium–silver tube. The bleed and product streams leaving the cell are cooled to

---

[1] To whom correspondence should be addressed.

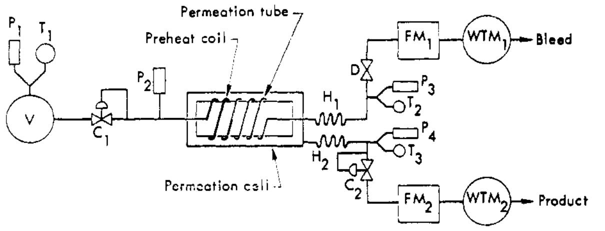

Figure 1. Schematic diagram of experimental apparatus

P, pressure transducers; T, chromel-alumel thermocouples; C, pressure control valves; D, microneedle valve; FM, hot wire anemometer, mass flowmeter; WTM, wet-test meter; H, cooling coils; V, supply volume

room temperature by cooling coils H_1 and H_2. The bleed system maintains a hydrogen sweep to prevent buildup of impurities on the inner surface of the palladium–silver tube. Valve D is used to set bleed flow rate. Bleed gas pressure is measured by P_3. Product gas back pressure is set by pressure control valve C_2 and measured by P_4. Flowmeters FM_1 and FM_2 monitor bleed and product flows. The quantity of bleed and product gas is measured by wet test meters WTM_1 and WTM_2. Eight thermocouples are installed in and around the permeation cell. The permeation temperature is calculated by averaging readings of three thermocouples installed within the permeation cell. Two parts of the equipment have been left out of the diagram: an oxygen-purge system to burn possible poisons from the palladium–silver tube surfaces; and a vacuum system for cleanup and outgassing of the system.

Figure 2, a partial cross section of the permeation cell, shows some details of construction. The preheat tube and the palladium–silver tube are wrapped around a core heated by four electrical resistance heaters. Note that the palladium–silver tube is wound as a double coil so that one end is free to move during temperature changes. Type 315 stainless steel was used for all parts of the cell in contact with the permeating gas. The joints between the stainless steel tubing and the Pd-Ag tubing were vacuum-brazed, using a silver–copper–palladium alloy (Palcusil-10). Thermal insulation is provided by several layers of heat shields in an evacuated space between the cell shell and an outer pressure vessel (not shown), which for safety reasons surrounds the permeation cell. The permeating hydrogen passes from inside the palladium–silver tube, through the tube wall, and into the annulus between core and shell before flowing out of the cell.

The active length of the tube is 229.3 ± 0.5 in., the outside diameter is 0.05 ± 0.0002 in., and the wall thickness is 0.0049 ± 0.0001 in. The tube was manufactured by Engelhard Industries of Alloy 349, which consists of palladium with 25 ± 0.5 wt % silver. The density of the alloy is 11.638 ± 0.004 g/cc.

Poisoning. Several precautions were taken to prevent poisoning of the palladium–silver surface. During assembly, care was taken to exclude lubricants or other materials which can poison the permeation tube. Valves with bellows seals and metal seats were employed upstream of the permeation cell. Elsewhere, valves with Teflon trim were used. Only metal seals are placed in heated regions. Before the permeation measurements, the tube was activated by an oxygen purge at 450°C for 15 min followed by outgassing and a hydrogen soak. The activation was repeated until a constant permeation rate was measured. Activation was also repeated every 10 to 12 experiments. The gases used in the experiment were hydrogen of 99.999% minimum purity. Impurities were O_2, N_2, CH_2, all less than 1 ppm with H_2O at 5 ppm. Deuterium was of 99.7% minimum purity. Impurities other than H_2 were less than 5 ppm.

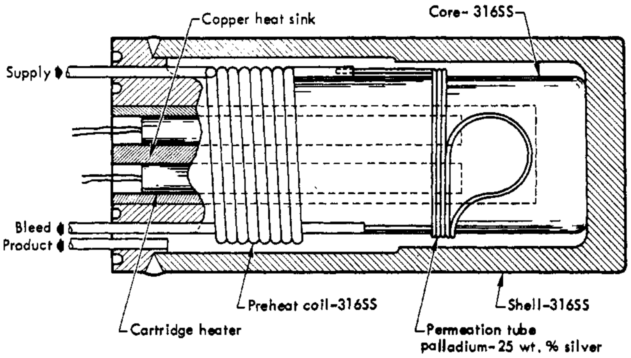

Figure 2. Details of permeation cell

Calibration. In preparation of the experimental equipment, three types of calibration were performed. Pressure transducers were calibrated with Heise gauges resulting in driving pressure readings with ±5 psi and back pressure measurements within ±1 psi. Mass-flow and wet-test meters were calibrated with a standard wet-test meter resulting in a volume reading within ±2%. Metal-sheathed iron-constantan thermocouples were calibrated with a standard centigrade thermometer, resulting in a reading within ±2°C at room temperature.

The temperature of permeation was the most difficult variable to measure. Accurate measurement of temperature had two problems: accuracy of the thermocouples used and measurement of a representative permeation temperature. It was impossible to calibrate the installed thermocouples above room temperature, and, measurements at 500°C could be in error by as much as ±10°C. Placement of thermocouples to obtain a truly representative diffusion temperature was difficult. Due to the somewhat fragile nature of the tube, it was not desirable to attach thermocouples to the coil itself. The thermocouples placed around the coil were influenced by temperature gradients in the cell. Due to the problems of calibration and temperature gradients, the three thermocouples which were used to measure permeation temperature showed a spread of 15° at 400°C.

The permeation temperature for each experiment was determined by averaging the readings from three thermocouples taken over the period of the experiment. The change in temperature over the course of an experiment was less than 5°C.

Evaluation of the above indicates that the measured permeation temperatures have a precision of ±8°C, but only an accuracy within ±15°C. An uncertainty of ±15°C introduces a maximum uncertainty of only ±4% in the permeation rate.

Procedure. Permeation measuremente were made by presetting the conditions (*i.e.*, temperature, driving pressure back pressure, bleed flow rate) and allowing flows to stabilize before taking data. The data from four pressure transducers, 11 thermocouples, two flowmeters, and two wet-test meters are automatically recorded at 4-sec intervals by a PDP-8/S computer. The data are normally recorded over a 5-min period. *PVT* calculations were made using the Redlich-Kwong equation of state by the method of Chueh and Prausnitz (*3*).

The bleed rate for most experiments was approximately 0.05 mol/min. Measured permeation rates should not be affected by bleed rate as long as it is sufficient to prevent buildup of impurities next to membrane surface. This was verified by three experiments made with a bleed rate of 0.08 mol/min. The measured permeation rates agree, within experimental error, with similar experiments at a bleed rate of 0.05 mol/min.

RESULTS AND DISCUSSION

Hydrogen and deuterium permeation measurements have been made at nominal temperatures of 300°, 400°, and 500°C and at driving pressures to 1000 psia. The results are given in Table I for hydrogen and Table II for deuterium. To show how the results correlate with pressure, the data are plotted as $R/\exp(b/T)$ *vs.* $(P_H^{1/2} - P_L^{1/2})$. The experimentally measured rate, R, is divided by the exponential temperature term to minimize scatter due to temperature differences between experiments. The constant, b, is experimentally determined and will be discussed below. Figures 3, 4, and 5 show the results for hydrogen permeation and for deuterium permeation at 300°, 400°, and 500° C, respectively.

Table I. Hydrogen Experiments

Product rate, mol/min	Temp, °C	Press., psia	Back pressure, psia
0.525	307	1003	27
0.450	280	986	22
0.503	304	1003	21
0.503	296	1000	20
0.393	300	1001	99
0.361	293	1016	101
0.367	292	999	101
0.457	293	806	20
0.329	294	807	102
0.401	306	491	18
0.362	287	514	19
0.378	293	511	19
0.261	301	494	99
0.234	284	533	100
0.244	293	513	102
0.244	296	201	17
0.232	284	213	17
0.239	294	210	18
0.103	295	202	98
0.100	288	218	100
0.106	300	217	102
0.697	401	984	22
0.691	409	990	22
0.683	403	977	22
0.661	391	986	22
0.654	394	1005	24
0.633	376	1006	23
0.619	362	1030	23
0.652	387	1000	22
0.683	421	982	23
0.664	394	1014	22
0.682	400	1015	22
0.605	378	1000	50
0.640	406	1037	51
0.523	367	1004	98
0.561	394	1039	101
0.616	410	802	21
0.572	405	816	49
0.484	398	784	98
0.493	400	837	102
0.468	383	799	101
0.481	419	498	19
0.427	411	500	49
0.418	391	518	15
0.357	401	513	99
0.339	389	513	101
0.347	397	299	18
0.292	395	308	50
0.283	392	312	51
0.212	396	302	100
0.216	393	322	101
0.264	383	214	17
0.139	401	94.2	16
0.075	406	96.2	48
0.752	479	993	23
0.646	486	994	99
0.626	485	1014	100
0.513	480	506	20
0.379	481	502	100
0.373	477	522	100
0.277	473	203	17
0.125	482	199	99
0.124	481	210	98

Table II. Deuterium Experiments

Product rate, mol/min	Temp, °C	Press., psia	Back pressure, psia
0.394	308	1001	22
0.395	295	1010	20
0.278	304	498	20
0.251	297	512	49
0.349	395	509	49
0.199	310	515	100
0.158	301	208	18
0.123	294	212	50
0.122	300	206	50
0.128	300	215	50
0.076	305	213	99
0.460	400	1001	23
0.460	385	1031	23
0.303	381	504	20
0.336	403	516	19
0.302	398	520	49
0.299	399	515	51
0.210	381	478	101
0.162	380	207	18
0.180	407	211	19
0.139	420	209	50
0.135	399	209	50
0.078	382	214	99
0.512	508	1004	24
0.339	501	515	21
0.339	509	509	48
0.330	489	523	52
0.246	498	508	100
0.167	498	203	23
0.152	521	209	51
0.145	484	212	51
0.078	499	205	100

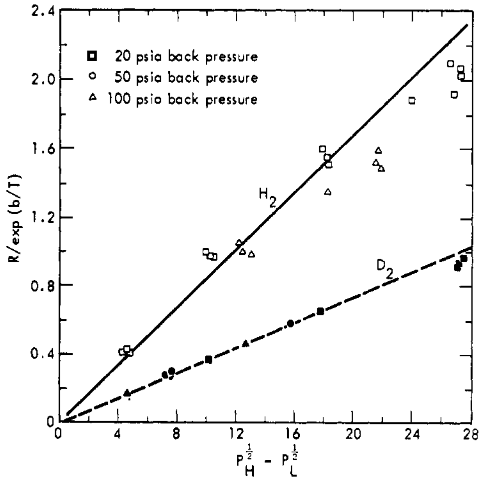

Figure 3. Hydrogen and deuterium permeation at 300°C

The plotted data should be a straight line if the $(P_H^{1/2} - P_L^{1/2})$ term adequately represents the pressure dependence. The data do fall on a straight line for hydrogen at 500°C and for deuterium at 400° and 500°C. The plot for hydrogen at 300°C is curved, with the 20 psia back-pressure points on a distinctly different curve from the 100 psia back-pressure points. The results for hydrogen at 400°C show much less curvature with all points close to the same curve. Deuterium, at 300°C, lies on a straight line if the three experiments at 1000 psia driving pressure are ignored. The deviation from straight line dependence at 300°C is as expected, since Hickman's

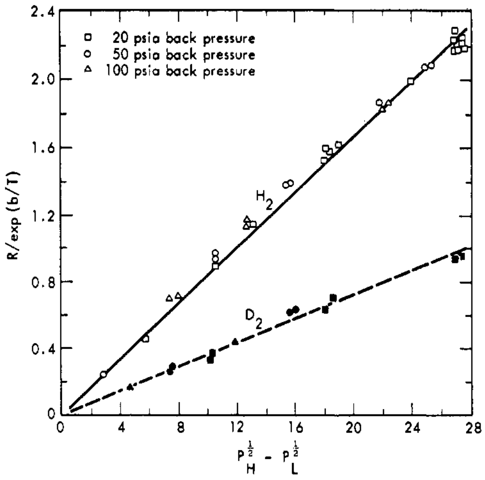

Figure 4. Hydrogen and deuterium permeation at 400°C

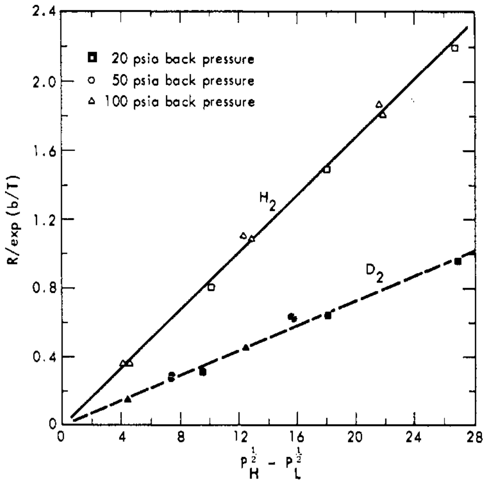

Figure 5. Hydrogen and deuterium permeation at 500°C

solubility experiments show a similar deviation from $P^{1/2}$ dependence in the same region (*6*).

Constants *a* and *b* of Equation 4 were determined by a least-squares fit to the data. For curve-fitting purposes, all the results for hydrogen at 300°C were omitted, while for deuterium, only the results at 1000 psia and 300°C were omitted. The resulting equation for hydrogen is:

$$R = 3.85 \times 10^{-6} A \exp(-794/T) \times (P_H^{1/2} - P_L^{1/2})/h \text{mol/min} \quad (5)$$

and the resulting equation for deuterium is:

$$R = 1.68 \times 10^{-6} A \exp(-479/T) \times (P_H^{1/2} - P_L^{1/2})/h \text{mol/min} \quad (6)$$

where A is the effective area of membrane, cm²; T is the temperature, °K; h is the thickness of membrane, cm; P_H is the driving pressure, psia; and P_L is the back pressure, psia.

These equations have been plotted as a straight line in Figures 3 through 5 in order to compare them with the data. All but hydrogen at 300°C are represented quite well.

Figure 4 includes 11 hydrogen permeation experiments, all nominally at the same conditions: 400°C, 1000 psia driving pressure and 20 psia back pressure. These experiments were performed at various times during the period of experimentation and were used as control experiments to check for poisoning. Several control experiments were performed following a series of experiments without a purge; the rest were performed immediately after an oxygen purge. Slight increases in permeation rate were observed following the purge; these were less than experimental error and may be spurious. All the control experiments agreed within ±3%.

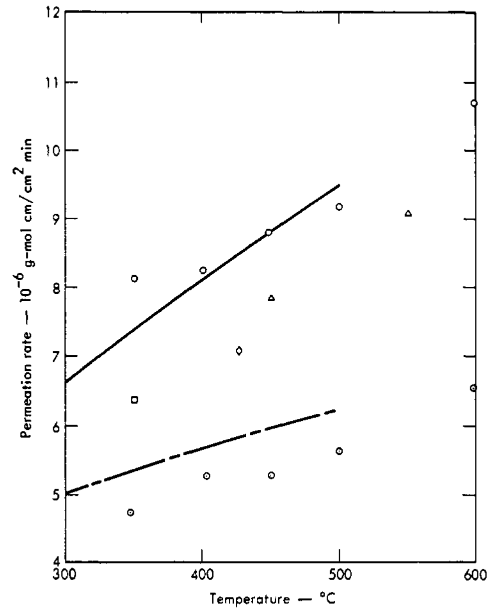

Figure 6. Comparison of hydrogen and deuterium permeation measurements through palladium

25 Wt % silver at P_H = 114.7 psia, P_L = 14.7 psia
—— (H_2) Equation 5
– – – (D_2) Equation 6
○ (H_2) Rubin (*15*)
⊙ (D_2) Rubin (*15*)
□ (H_2) McKinley (*14*)
△ (H_2) Hunter, foil (*10*)
◇ (H_2) Hunter, tube (*9*)

A comparison of our results with those of other investigators is shown in Figure 6 for conditions of 115 psia driving pressure and 14.7 psia back pressure. The importance of comparison at identical pressures and back pressures has been pointed out by Hunter (*8*). The hydrogen data are very close to that of Rubin (*15*), but the deuterium data are not quite so close. McKinley's data (*14*) have been extrapolated to these conditions from two measurements at 350°C: one at P_H = 90 psia, P_L = 14.7 psia, the other at P_H = 315 psia, P_L = 14.7 psia, using the $P_H^{1/2} - P_L^{1/2}$ relationship. Hunter's data for a Pd-Ag tube at T = 427°C (600°F), P_H = 115 psia, is 18% below ours. However, at P_H = 415 psia, the difference is only 8% (*9*).

In general, the agreement in Pd-25 Ag data is much better than is the case for pure palladium, where differences of several orders of magnitude have been reported (*11*). Some of the differences observed in Figure 6 may be due to the difficulty in accurately determining the area/thickness ratio.

Poisoning of the Pd-Ag surface must also be considered, since this has been shown by David (*5*) to be the cause of disagreement in pure palladium data. There have been several excellent discussions of poisoning (*5*, *16*, *18*), so we will mention only briefly one aspect to the problem.

Determining surface poisoning is difficult. The usual supposition is that permeation is not surface controlled $P^{1/2}$ dependence is observed. This is not a clear test. Barrer has shown that apparent $P^{1/2}$ dependence is possible under surface controlled conditions (*1*, *2*). Partial poisoning of the surface can reduce the permeation rate while still exhibiting $P^{1/2}$ dependence over moderate ranges of pressure. We believe our permeation measurements to be on essentially unpoisoned palladium-silver surfaces for several reasons: Care is taken to prepare and maintain clean palladium–silver permeation tubes; $P^{1/2}$ dependence is present over a wide range of pressure; and the measured permeation rates, when compared with those of other investigators, are close to the highest observed under the same conditions.

LITERATURE CITED

(1) Ash, R., Barrer, R. M., *Phil. Mag.*, **4**, 1197-1206 (1959).
(2) Barrer, R. M., *ibid.*, **28**, 353 (1939).
(3) Cheuh, P. L., Prausnitz, J. M., *Ind. Eng. Chem. Fundam.*, **6**, 429 (1967).
(4) Darling, A. S., *Proc.*, "Symposium on Less Common Means of Separation," Institute of Chemical Engineers, Birmingham, England, April 1963.
(5) Davis, W. D., *Knolls Atomic Power Laboratory, Rept.*, **KAPL-1375** (1955).
(6) Hickman, R. G., *J. Less-Com. Metals*, **19**, 369–83 (1969).
(7) Hickman, R. G., Lawrence Radiation Laboratory, Livermore, Calif., private communication (1969).
(8) Hunter, J. B., J. Bishop and Co. Platinum Works, Malvern, Pa., private communication (1971).
(9) Hunter, J. B., "Ultrapure Hydrogen by Diffusion Through Palladium Alloys," presented at the Symposium on Production of Hydrogen, Petrol. Div., ACS Meeting, New York, N.Y., Fall 1963; published in *Am. Chem. Soc., Div. Petrol. Chem., Prepr.*, 8(4), B49-B60 (1963).
(10) Hunter, J. B., U.S. Patent 2,773,561 (Dec. 11, 1965).
(11) Hurlbert, R. C., Konecny, J. O., *J. Chem. Phys.*, **34**, 655-8 (1961).
(12) Jost, W., "Diffusion in Solids, Liquids, Gases," p 2, Academic Press, New York, N.Y., 1960.
(13) Lewis, F. A., "The Palladium Hydrogen System," *ibid.*, 1967.
(14) McKinley, David, U.S. Patent 3,247,648 (April 26, 1966).
(15) Rubin, L. R., *Tech. Bull.*, Vol. 7, Engelhard Industries, Inc., Newark, N.J., 1966.
(16) Salmon, O. N., Randall, D., Wilk, E. A., *Knolls Atomic Power Laboratory Rept.*, **KAPL-1674** (November 1956).
(17) Sieverts, A., Krumbhaar, W., *Ber. Deut. Chem. Ges.*, **43**, 893 (1910).
(18) Van Swaay, M., Birchenall, C. E., *Trans. Met. Soc. AIME*, **218**, 285-9 (1960).

Received for review January 21, 1971. Accepted August 19, 1971. Work supported by the U.S. Atomic Energy Commission.

Specific Conductance of Concentrated Solutions of Magnesium Salts in Water-Ethanol System

JERRY F. CASTEEL and EDWARD S. AMIS[1]
Chemistry Department, University of Arkansas, Fayetteville, Ark. 72701

The equivalent conductances of dilute solutions of magnesium sulfate in water–ethanol solvents at 25°, 35°, and 45°C were presented in a previous paper. This work is an extension of that paper into the highly concentrated region. The specific conductance of concentrated solutions of magnesium sulfate were measured at 25°, 35°, and 45°C in pure water and in 20.1 and 40.7 wt % ethanol. An empirical equation is presented which fits the data well over the range of solvent compositions and temperatures studied. The empirical equation which relates the specific conductance at the maximum and the corresponding concentration at different solvent compositions and different temperatures is tested using the data presented here and that of Than and Amis for concentrated solutions of magnesium chloride in water–ethanol solvents at 25°, 35°, and 45°C.

Interest in the conductivity of concentrated solutions has increased greatly in the last few years; however, a satisfactory relationship between the specific conductance, L, and the concentration, C, has yet to be formulated which will work over a range of electrolytes, solvents, and temperatures. Than and Amis (*5*) presented an equation for magnesium chloride which gave good results over the range of concentrations, solvents, and temperatures studied. Their equation has the form of a modified normal distriution and is given by Equation 1.

$$L = L_m e^{-A(C-\mu)^2} \tag{1}$$

where

L = specific conductance
L_m = maximum specific conductance
C = concentration (moles/kg of solution)
μ = concentration corresponding to the maximum specific conductance
A = constant

To test the significance of L_m and μ as important parameters in the conductance of concentrated solutions of electrolytes, the specific conductance of the bi-bivalent electrolyte, magnesium sulfate, was measured in the water–ethanol system at 25°, 35°, and 45°C. The equivalent conductances of dilute solutions of magnesium sulfate in water–ethanol solvents were reported in an earlier paper (*2*).

EXPERIMENTAL

All weights were previously standardized against NBS weights. The solutions were made up by weight corrected to vacuum using a Seederer and Kohlosbush 3-kg capacity balance with an average sensitivity of one division per 10 mg. The temperatures of the thermostated oil baths were held to ±0.01°C at 25°, 35°, and 45°C. Beckmann thermometers which had been previously standardized against and an NBS certified thermometer were used to read the bath temperatures. The densities of the mixed solvents were determined with a calibrated arm-pycnometer. The solvent compositions were

---

[1] To whom correspondence should be addressed.